Current Biology, Vol. 13, 1679–1686, September 30, 2003, ©2003 Elsevier Science Ltd. All rights reserved. DOI 10.1016/j.cub.2003.08.034

Intraflagellar Transport Is Required in *Drosophila* to Differentiate Sensory Cilia but Not Sperm

Young-Goo Han,[1,2] Benjamin H. Kwok,[3,4] and Maurice J. Kernan[2,3,*]
[1]Graduate Program in Genetics
[2]Center for Developmental Genetics
[3]Department of Neurobiology & Behavior
State University of New York at Stony Brook
Stony Brook, New York 11794

Summary

Background: Intraflagellar transport (IFT) uses kinesin II to carry a multiprotein particle to the tips of eukaryotic cilia and flagella and a nonaxonemal dynein to return it to the cell body. IFT particle proteins and motors are conserved in ciliated eukaryotes, and IFT-deficient mutants in algae, nematodes, and mammals fail to extend or maintain cilia and flagella, including sensory cilia. In *Drosophila*, the only ciliated cells are sensory neurons and sperm. *no mechanoreceptor potential* (*nomp*) mutations have been isolated that affect the differentiation and function of ciliated sense organs. The *nompB* gene is here shown to encode an IFT protein. Its mutant phenotypes reveal the consequences of an IFT defect in an insect.
Results: Mechanosensory and olfactory neurons in *nompB* mutants have missing or defective cilia. *nompB* encodes the *Drosophila* homolog of the IFT complex B protein IFT88/Polaris/OSM-5. *nompB* is expressed in the ciliated sensory neurons, and a functional, tagged NOMPB protein is located in sensory cilia and around basal bodies. Surprisingly, *nompB* mutant males produce normally elongated, motile sperm. Neuronally restricted expression and male germline mosaic experiments show that *nompB*-deficient sperm are fully functional in transfer, competition, and fertilization.
Conclusions: NOMPB, the *Drosophila* homolog of IFT88, is required for the assembly of sensory cilia but not for the extension or function of the sperm flagellum. Assembly of this extremely long axoneme is therefore independent of IFT.

Introduction

The eukaryotic cilium or flagellum is a distinct subcellular compartment, with its own characteristic microtubular cytoskeleton, the axoneme, and a membrane that, though continuous with the plasma membrane, can localize distinct sets of proteins. This distinction is maintained by a specific mechanism of intraflagellar transport (IFT). IFT was first observed in the single-celled alga *Chlamydomonas* as a bidirectional movement of uniformly sized particles along the flagellum, in the space between the axoneme and the flagellar membrane [1]. Biochemical characterization of the particles revealed over 16 constituent proteins associated in A and B subcomplexes [2, 3]. Particle movement toward the plus ends of the axonemal microtubules at the tip of the flagellum is driven by kinesin II [2], and mutants lacking kinesin II subunits or complex B proteins do not extend cilia beyond the transition zone of the basal body. In mutants that express a temperature-sensitive kinesin, flagella shrink after a shift to the restrictive temperature, and this shrinkage indicates that IFT is needed to maintain and regulate flagellar length [2, 4, 5]. IFT particles and kinesin are returned to the cell body by a nonaxonemal dynein, and mutants with defects in this process [6, 7] typically have swollen cilia that accumulate IFT particles. Some IFT proteins are concentrated in the cytoplasm close to the basal bodies as well as in the cilia proper, and the transition fibers that connect the basal body to the cell membrane are a possible site for the docking and exchange of IFT particles, motors, and cargo [8].

IFT proteins and motors are well conserved in ciliated eukaryotes, including nematodes and mammals [9]. Mutations affecting IFT motors and particle proteins in these organisms cause a variety of developmental and functional defects, many of which are traceable to missing or defective cilia. The nematode *Caenorhabditis* has ciliated sensory neurons in which IFT particle transport has been visualized [10]. Many mutations isolated due to defects in sensory function or ciliary differentiation [11, 12] affect IFT complex proteins or motors [13–18] or an RFX-type transcription factor that regulates expression of several IFT genes [19].

Single "primary" cilia are nearly ubiquitous in mammalian cells [20] and are overtly differentiated for a sensory role in photoreceptors. Cilia with a central pair of microtubules (9+2 configuration) occur as sperm flagella and in polyciliated cells that line airway and brain epithelia. Primary cilia, sensory cilia, and motile cilia all contain IFT proteins, and mutations affecting IFT in mammals are pleiotropic, reflecting ciliary roles in development and in transducing sensory and regulatory signals [21]. For instance, Polaris, the mouse homolog of IFT88, is present in primary cilia, motile cilia, and sperm. Mice homozygous for a hypomorphic allele, *Tg737*^{orpk} [22], have defects including kidney cysts, photoreceptor degeneration, skeletal abnormalities, and spermatogenesis defects [23–25] (J.T. San Agustin, G.J. Pazour and G.B. Witman, personal communication). A targeted *Tg737* knockout is embryonic lethal, with early embryonic defects that include randomized left/right asymmetry, a consequence of missing cilia on the embryonic ventral node [26]. The defective cilia in kidney tubules of *orpk* mutant mice [27] were in fact the first indicator that undifferentiated primary cilia have important physiological functions [28]. The similarity of some IFT proteins to signaling and regulatory proteins found elsewhere in the cell further suggests that IFT may be involved in coupling cilia-mediated signals to intracellular pathways [9].

In *Drosophila*, cilia are found in Type I, monodendritic

*Correspondence: mkernan@notes.cc.sunysb.edu
[4]Present address: Laboratory of Chemistry and Cell Biology, Rockefeller University, New York, New York 10021.

sensory neurons in which 9+0-type cilia located at the distal tip of sensory processes transduce mechanical or chemical sensory stimuli. Insect photoreceptors are not ciliated, but flies, unlike nematodes, do have flagellated sperm with a canonical 9+2 axoneme and accessory tubules. Ciliogenesis-defective mutants of *Drosophila* are therefore expected to combine sensory and spermatogenesis defects. We show that the *nompB* gene, previously identified by behavioral and electrophysiological mutant defects, encodes the *Drosophila* counterpart of *Chlamydomonas* IFT88, *Caenorhabditis* OSM-5, and mammalian Polaris/Tg737. We find that *nompB* mutants have defects in sensory cilia that are consistent with a loss of IFT and that the NOMPB protein is located in cilia and around basal bodies. Surprisingly, it has no role in sperm differentiation or function.

Results and Discussion

Ciliary Defects in *nompB* Mutants

Three *nompB* alleles were isolated in a genetic screen for defects in mechanosensory behavior and electrophysiology [29]. All three alleles showed the same phenotype when homozygous: severe uncoordination, associated with a complete loss of transduction in mechanosensory bristles [29] and in auditory chordotonal organs [30]. Similar phenotypes were seen in flies carrying two different mutant alleles and in flies hemizygous for a mutant allele. Both of these types of sense organs are innervated by one or more sensory neurons surrounded by specialized supporting cells. Each neuron has a single sensory process, divided into a proximal inner segment and a distal outer segment [31]. The outer segment is a modified cilium that extends from the more distal of a pair of basal bodies located at the tip of the inner segment. In mechanosensory neurons, it is connected to stimulus-transmitting structures by an extracellular dendritic cap and is thought to be the site of transduction.

We visualized neurons of campaniform sensilla, external sense organs similar to bristles, by expressing a green fluorescent protein (GFP) in neurons. In *nompB* mutants, neuronal cell bodies and axons appeared normal, but the sensory process that normally contacts the dome-shaped sensillum was retracted (Figures 1A–1D). To study ciliary morphology in more detail, we examined the longer cilia of chordotonal neurons expressing a membrane-associated green fluorescent protein (mCD8-GFP) (Figures 1E–1H). Wild-type chordotonal organs of the femur and antenna include pairs of sensory neurons, each bearing a single cilium that bears a characteristic ciliary dilation. In *nompB* mutants, cilia were absent, while a few short, thin, irregularly curved processes remained on some neurons. The defect was limited to the cilia: inner segments and cell bodies appeared normal, and the aberrant processes extending from *osm-5* mutant cell bodies [12, 18] were not seen in *nompB* mutants. Cilia were also missing from all olfactory neurons of the third antennal segment (Figures 1I and 1J). Thus, a general defect in the differentiation of sensory cilia underlies the behavioral and electrophysiological defects of *nompB* mutants.

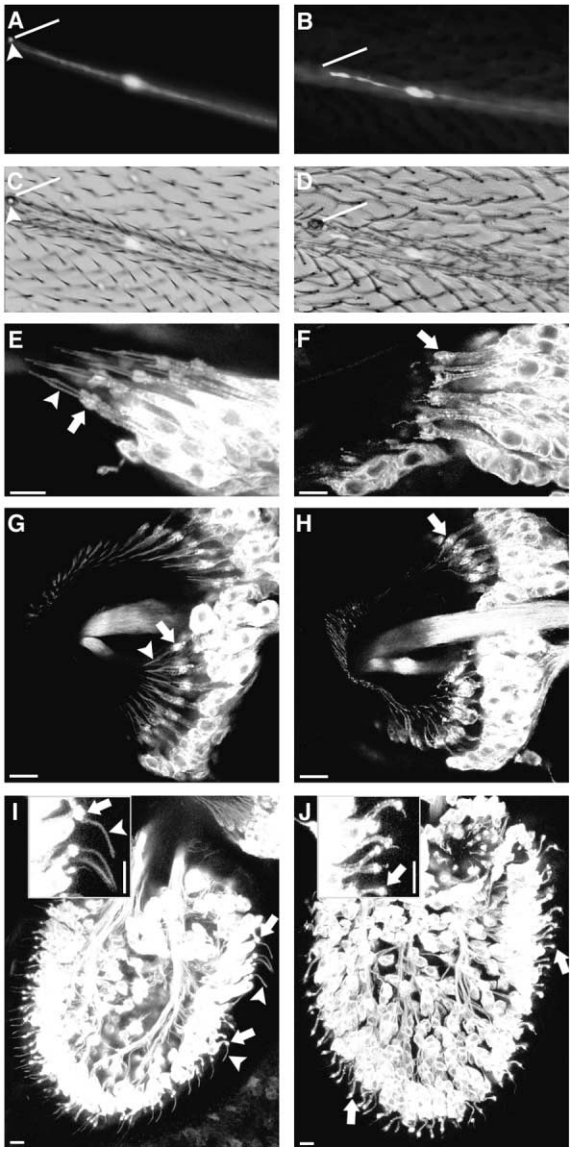

Figure 1. Defective Sensory Cilia in *nompB* Mutants

(A–J) Neurons and sensory processes in (A, C, E, G, and I) wild-type and (B, D, F, H, and J) *nompB* mutant flies were visualized by targeted expression of green fluorescent proteins. (A–D) Campaniform sensilla on the wing vein. The dilated ciliary tip of the sensory process (arrowhead), normally located under the dome of the sensillum (line) (A and C), is missing in the mutant (B and D). (E–H) Sensory neurons in the (E) femoral and (G) antennal chordotonal organs have cilia that are missing or deformed in the mutant (F and H). (I and J) Olfactory neurons on the third antennal segment, showing long cilia (inset) in wild-type, that are missing or truncated in the mutant. The arrows (E)–(J) indicate the distal ends of inner dendritic segments, and the arrowheads indicate the ciliary outer segments that extend from them.

Positional Cloning of *nompB*

nompB was mapped to cytogenetic position 39E7-F1 by deficiency complementation tests and by P element-induced male recombination [32]. The minimal interval containing *nompB* was delimited proximally by the P element insertion *l(2)02074* and distally by the breakpoint of a deletion, *Df(2L)03832MR1*, that was generated

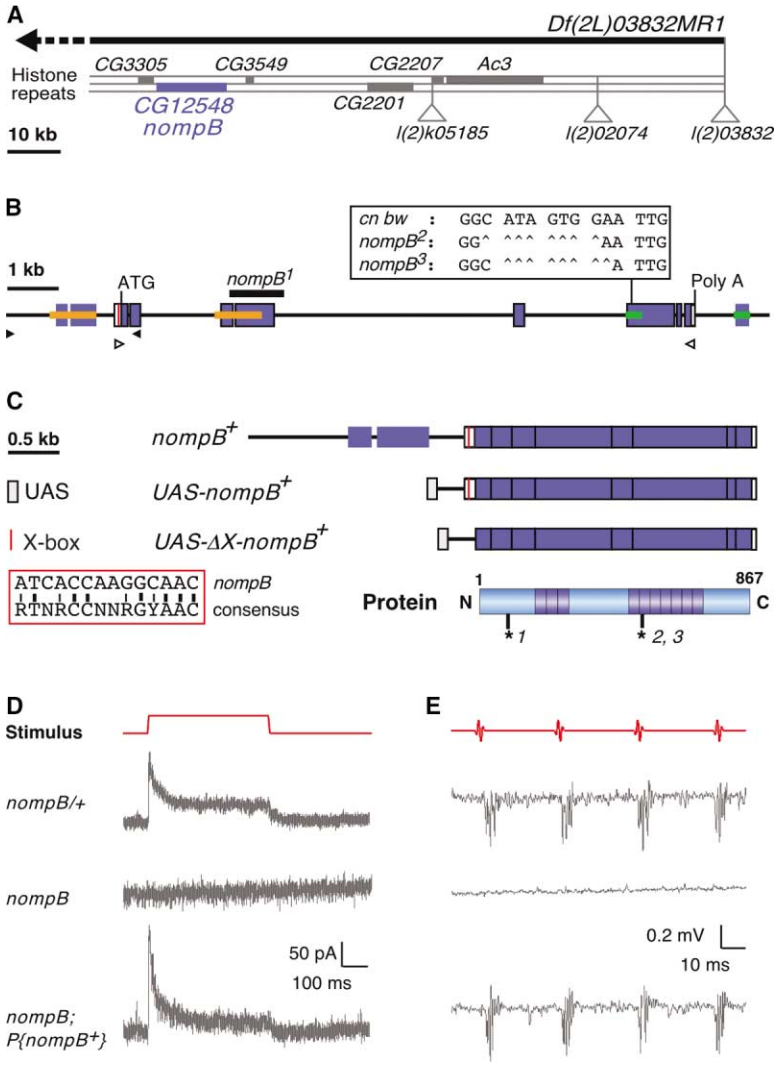

Figure 2. Gene Identification and Structure

(A) Molecular maps of the *nompB* region, showing known and predicted genes, P insertion sites, and the *Df(2L)03832MR1* deletion. The distal breakpoint of *Df(2L)03832MR1* is located in a histone repeat array, but its exact location has not been defined.

(B) Genomic structure and mutant alleles of *nompB*. Exons are shown as blue boxes. Overlapping orange and green bars indicate sequences that are duplicated upstream and downstream of the gene. The 1100 bp deletion in *nompB*^{1} is shown as a black bar. The overlapping 8 bp deletions in *nompB*^{2} and *nompB*^{3} are shown in a box; both lead to an identical frameshift and a truncated protein. Primers used to amplify the upstream genomic region and full-length cDNA are indicated by closed and open triangles, respectively.

(C) Transgene constructs described in the text, aligned with the encoded protein. The X box, a putative regulatory motif in the 5′-UTR, is shown as a red line in the constructs and is aligned with the consensus X box sequence in the inset. The dark blue boxes in the protein indicate tetratricopeptide repeat (TPR) motifs; the numbered asterisks indicate the predicted truncation sites for each mutant allele.

(D and E) Transgenic rescue of the *nompB* electrophysiology defects in bristles and chordotonal organs. (D) Bristle mechanoreceptor currents in response to a step stimulus in a *nompB*/+ heterozygote, a *nompB*/*Df* hemizygote, and a hemizygote with a P insertion carrying the genomic-cDNA fusion in Figure 2C. (E) Antennal sound-evoked potentials recorded from the same genotypes.

from the P element insertion *l(2)03832*. The *Df(2L)03832MR1* deletion breakpoint falls in a histone gene repeat array. Although the published *Drosophila* genome sequence [33] does not extend to these repeats, it does include an approximately 100 kb segment that includes six predicted genes distal to the *l(2)02074* insertion site. Among these, CG12548 was identified as a possible *nompB* candidate due to its similarity to the mammalian *Tg737* gene.

The previously predicted structure of CG12548 was ambiguous due to two near-exact partial duplications of internal exons that flank the gene proper (Figure 2B). By TBLASTN alignment with the putative mammalian homolog, we adjusted the predicted structure to exclude the duplicated exons and include exon 3. RT-PCR and sequencing of overlapping cDNA segments confirmed this structure and identified a single alternatively spliced exon. The longer isoform contains an open reading frame that begins in exon 1, following two in-frame stop codons, and encodes 867 amino acids. The shorter isoform lacks the 29 amino acids encoded by exon 7. The first exon follows a highly predicted promoter sequence and includes a putative binding site for an RFX-type transcription factor, a probable transcriptional regulator of IFT genes [19, 34]. The 5′ flanking duplication was not included in any transcript detected by RT-PCR.

To verify the identity of CG12548 with *nompB*, we sequenced exons from all three *nompB* mutant alleles and the *cn bw* stock from which they were derived and found independent alterations in each allele. In *nompB*^{1}, an approximately 1 kb deletion removes exon 4 and part of exon 3. RT-PCR from *nompB*^{1} mutants showed that this results in the missplicing of exon 2 to exon 5 and a frameshift at amino acid 109 that yields a 110 amino acid-truncated protein. *nompB*^{2} and *nompB*^{3} have overlapping but distinct 8 base deletions in exon 6. These deletions result in the same frameshift and premature stop codon in the middle of the gene and thus yield a 542 amino acid-truncated protein with 12 novel C-terminal amino acids. Notably, none of the alterations found in *nompB* alleles were the single-base transitions expected from the ethylmethanesulfonate mutagenesis in which they were isolated, although at least ten other mutations isolated from the same screen [35, 36] (and our unpublished data) are transitions. However, all three

alterations either overlap or fall within the two gene segments that are present in wild-type sequences as flanking duplications; this finding suggests that the *nompB* mutations resulted from duplication-initiated rearrangements.

To confirm the identity of CG12548 and *nompB*, we made a functional *nompB* transgene by amplifying a full-length cDNA including the translation start site, alternate exon 7, and the polyadenylation signal and joining it to a 2.2 kb fragment of upstream genomic DNA (Figure 2D). Twelve independent P element inserts containing this construct rescued the behavioral (data not shown) and electrophysiological defects of *nompB* mutants in germline transformants (Figures 2D and 2E).

Conservation of NOMPB and Other IFT Proteins

The predicted NOMPB protein shows 28%–33% amino acid identity and 47%–48% similarity with its homologs in *Chlamydomonas*, *Caenorhabditis*, and mammals. Like its homologs, NOMPB contains two groups of three and seven tetratricopeptide repeat (TPR) motifs: these are the most conserved parts of the protein. A TPR comprises 34 amino acids in a α-helical hairpin fold [37], and stacked TPRs form potential protein interaction sites [38, 39]. The protein predicted to be encoded by the $nompB^{1}$ allele lacks all the TPR motifs, while the $nompB^{2}$ and $nompB^{3}$ mutations truncate the protein in the fifth TPR.

NOMPB is the only IFT88 homolog encoded by the sequenced *Drosophila* genome. Other IFT particle proteins are also conserved in *Drosophila*, as in nematodes [40]: orthologs exist for the *Chlamydomonas* B complex proteins IFT172/*Caenorhabditis* OSM-1 (*Drosophila* predicted gene CG13809), IFT57/55/CHE13 (CG8553), IFT52/OSM-6 (CG9595), the *Caenorhabditis* B complex protein CHE-2 (CG9333), and the A complex proteins IFT140/CHE-11 (CG11838) and IFT122/DAF10 (CG7161). Of the known *Chlamydomonas* IFT particle proteins, only IFT20, a B complex protein that is present in vertebrates, appears not to be well conserved in the fly. *Drosophila* also contains homologs for IFT-associated kinesin II subunits (Klp64D, Klp68D, DmKAP) [41–43]. Thus, *Drosophila* appears to express most of the IFT components.

NOMPB Is Localized to Sensory Cilia

To investigate the subcellular localization of NOMPB, we joined GFP to the N terminus of NOMPB by inserting the GFP coding sequence in frame into the genomic-cDNA rescue construct (Figure 3A). The tagged gene rescued the behavioral defects of *nompB* mutants (data not shown), which showed that it is normally expressed and functional. In transgenic flies, GFP-NOMPB expression was observed only in type I, ciliated sense organs, including olfactory sensilla (Figures 3B), chordotonal organs (Figures 3C–3J), campaniform sensilla, and mechanosensory bristles (data not shown). In chordotonal organs, GFP-NOMPB weakly labels the neuronal cell bodies and inner segments and is enriched in the ciliary outer segments. Counterstaining with the monoclonal antibody 22C10 [44], which labels all parts of the neuron except the outer segment, confirms this localization and shows that GFP-NOMPB is most concentrated at the distal end of the inner segment, the location of the basal bodies (Figures 3E and 3F).

A winged-helix RFX transcription factor is specifically expressed in ciliated sense organs in both *Caenorhabditis* [19] and *Drosophila* [34, 45]. In nematodes, it regulates the expression of several IFT proteins, via a palindromic "X box" DNA sequence often located close to transcription start sites [19]. A canonical X box is located within the 5′-untranslated region of the *nompB* transcription unit. Mutants for either the *Caenorhabditis* (*daf-19*) [19] or *Drosophila* (*Rfx*) [46] RFX factor lack sensory cilia. GFP-NOMPB is undetectable in *Rfx* mutant flies (Figure 3G), confirming that *Rfx* is required for normal *nompB* expression.

Flies mutant for the kinesin II subunit Klp64D have missing or shortened cilia, as expected for an IFT defect [47] (and our unpublished data). In these mutants ($klp64D^{k1}/klp64D^{n123}$), some GFP-NOMPB is still present in the inner segment (Figures 3K–3M).

nompB Is Not Required for Spermatogenesis

Polaris, the mouse homolog of NOMPB, is expressed in immature spermatogonia, enriched in the mature flagellated sperm [24], and is required for spermatogenesis (J.T. San Agustin, G.J. Pazour, and G.B. Witman, personal communication). Because IFT is required for the normal assembly of all types of cilia and flagella, including mammalian sperm, we were surprised to observe that *Drosophila* males homozygous or hemizygous for each of the three *nompB* mutations produce individualized, motile sperm. The distribution of glycosylated proteins on sperm acrosome and tail was examined by using concanavalin A labeling [48] and was found to be normal (data not shown).

nompB mutant flies are too uncoordinated to mate, so it was not immediately evident if *nompB* mutant sperm are functional in fertilization. To test this, we generated male flies with normal behavior but *nompB*-defective sperm by targeted *nompB* expression and by generating germline mosaics. *nompB* cDNA constructs (Figure 2C) were selectively expressed under the control of the GAL4 enhancer trap system [49]. A construct using a full-length cDNA was able to rescue the sensory defect in the absence of any GAL4 driver, possibly due to the presence of an X box within the transcription unit. When 104 bp including the X box were deleted from the 5′-untranslated region of the cDNA, rescue of the sensory defects was dependent on the presence of neuronal GAL4 (data not shown). Rescued $nompB^{1}$/*Df(2L)03832MR1* mutant males carrying both the elav-GAL4 driver and the modified UAS-ΔX-$nompB^{+}$ construct were fertile, indicating normal sperm function.

In *Drosophila* females mated to multiple males, sperm from the last male to mate can displace and inactivate the sperm from previous males, so that most offspring are sired by the last male [50]. To test if *nompB* contributes to last-male sperm precedence, neuronally rescued *nompB* males and wild-type controls were used as second males following mating to a standard first male. The proportion of offspring (P_2) sired by neuronally rescued $nompB^{1}$/*Df(2L)03832MR1* second males (0.80) and con-

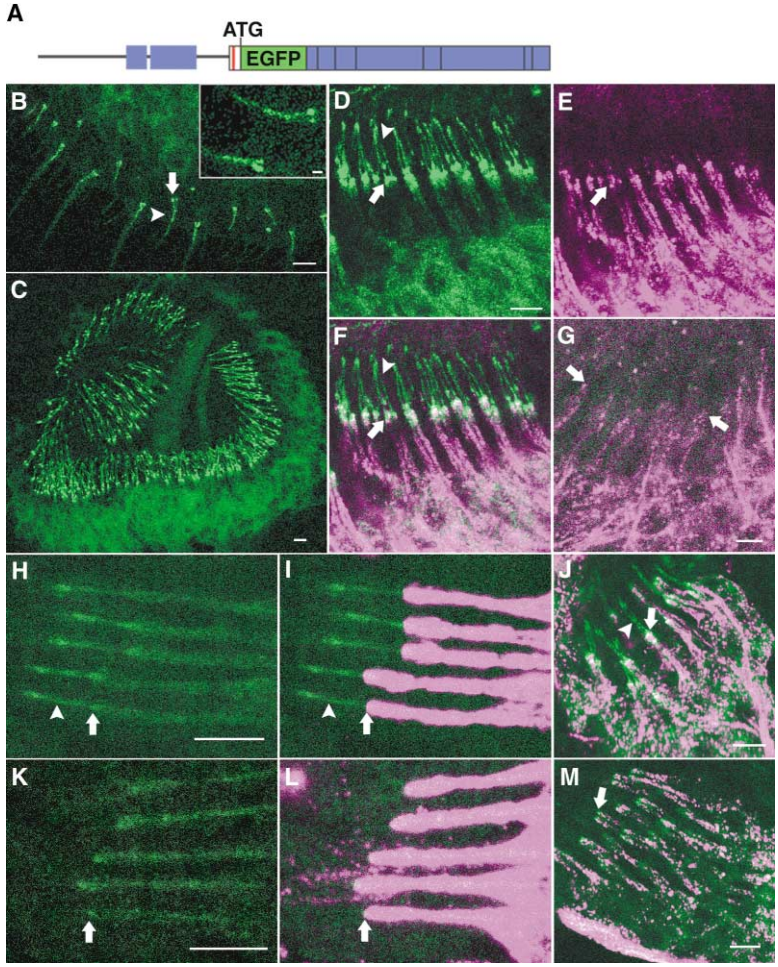

Figure 3. GFP-NOMPB Localization in Ciliated Sensory Neurons

(A) A sequence encoding enhanced GFP (EGFP) was inserted at the translation start site of the *nompB*$^{+}$ rescue construct to make a functional *GFP-nompB* fusion.

(B–M) Confocal images of sensory neurons expressing NOMPB-GFP (green) and counterstained with MAb22C10 (magenta). The arrows indicate the distal ends of inner segments, and the arrowheads indicate the ciliary outer segments. (B) Olfactory sensilla on the third antennal segment. The enlarged inset shows labeling in multiple olfactory neurons that extend cilia into a single bristle. (C–F) Antennal chordotonal organs showing (C and D) GFP labeling in ciliary outer segments and cell bodies, (E) labeling of inner segments with Mab22C10, and (F) a merged image. The GFP and 22C10 labeling overlap at the junction of the inner and outer segments. (G) In the antenna of *rfx*^{253}/*rfx*^{49} flies, no GFP-NOMPB signal is visible. (H–J) GFP-NOMPB in (H and I) wild-type embryonic and (J) adult femoral chordotonal organs. (K–M) The same organs in the kinesin-defective mutant *klp64D*^{k1}/*klp64D*^{n123}. Cilia are missing in the kinesin-defective mutant, but some GFP-NOMPB is still present in inner segments.

trol second males (0.85) did not differ significantly. The lack of *nompB* therefore does not affect the offensive competitive ability of sperm.

To address the possibility that a low level of expression either from the neuronal GAL4 driver or from the UAS constructs might be sufficient to support IFT in the germline, we generated homozygous *nompB* cells in heterozygous males by FRT-mediated mitotic recombination [51] (Figure 4A). Production of functional sperm from heterozygous germline cells was prevented by including a synthetic dominant, male sterile transgene, *P{HDM}*, encoding a fusion of the *Drosophila* dosage compensation protein MSL-2 to a bacterial DAM methylase (H. Oh and M. Kuroda, personal communication), on the *nompB*$^{+}$ chromosome. Male flies heterozygous for chromosomes carrying a *nompB* mutation and *P{HDM}* produce no motile sperm and are completely infertile (Figure 4B). When expression of a FLP recombinase was induced in this background, enabling FRT-mediated mitotic recombination to homozygose the *nompB* mutation, motile sperm and progeny bearing the *nompB* mutant chromosome were produced (Figure 4C).

Finally, the GFP-tagged NOMPB genomic construct that rescued the sensory defects showed no detectable GFP expression in the testis. Taken together, these data show that the *Drosophila* IFT88 homolog is not needed to assemble sperm flagella or for sperm motility, transfer, storage, competition, or fertilization. It is unlikely that there exists a separate, germline-specific IFT mechanism in *Drosophila*, as no other IFT88 homolog exists in the genome. Further support for the absence of IFT in fly sperm comes from *Drosophila* mutants defective in IFT-associated kinesin subunits, which show similar sensory defects and a similar lack of effect on spermatogenesis [47]. Mutations in *Drosophila* RFX, the transcriptional activator of several IFT genes, also cause defects in all sensory cilia, but not in spermatogenesis [46], even though RFX protein is present in late spermatid nuclei [34].

IFT is currently viewed primarily as an assembly mechanism that is required to construct any and all axonemal structures, including sperm flagella [21]; its absence from fly sperm is therefore unexpected. Two distinctive features of *Drosophila* spermatogenesis may be relevant to their lack of IFT. First, spermatids develop in a syncitial cyst and are not individually enclosed by plasma membrane until after the flagellar axonemes have fully elongated, so the growing tip of the axoneme is accessible from the cytoplasm [52, 53]. IFT particles, by contrast, are transported between the axoneme and a closely apposed ciliary membrane, a situation that does not exist in differentiating spermatids. Second, fly sperm flagella are extremely long: *D. melanogaster* sperm, at

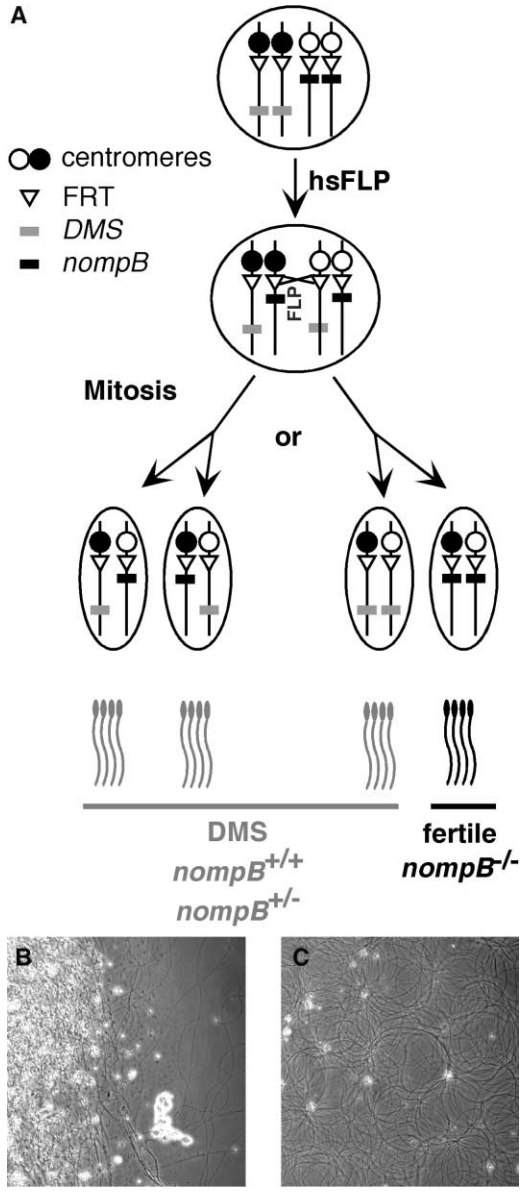

Figure 4. Generation of *nompB* Male Germline Mosaics

(A) The schematic shows chromosome arm 2L in a germline cell following chromosome duplication. One homolog carries a dominant, male sterile transgene (*DMS*, gray box), the other carries a *nompB* mutant allele (black box). Induction and action of the FLP recombinase causes recombination at the FRT sites; one mitotic segregation pattern yields a DMS^{-} $nompB^{-}$ daughter cell.

(B and C) Testis squashes from the *nompB/DMS; hsFLP* (B) without and (C) with FLP induction by heat shock. Motile sperm were seen only in the presence of an induced FLP. Males in which FLP expression was induced were fertile.

1.8–2.0 mm, are longer than the fly itself, and those of *D. bifurca* at over 50 mm in length [54] may be the longest axonemal structures. If conventional IFT cannot construct or maintain axonemes this long, selection for increased sperm length [55] may have favored other assembly mechanisms.

Conclusions

NOMPB is the *Drosophila* homolog of the IFT B complex protein IFT88/Polaris/OSM-5. Defects in the sensory cilia of *nompB* mutants, the localization of GFP-NOMPB to basal bodies and cilia, and the conservation of other IFT proteins in *Drosophila* all indicate that IFT is required in *Drosophila* sensory neurons for ciliary assembly. Surprisingly, the assembly and function of sperm flagella, the only other axonemal structure in the fly, are independent of NOMPB and probably independent of IFT.

Experimental Procedures

Drosophila Stocks, Culture, and Genetic Mapping

nompB mutant alleles were described previously [29]. Flies carrying inserts of the dominant, male sterile transgene *P{HDM = Hsp83P – DAM – MYC – MSL2}* on chromosome 2L were a gift from M. Kuroda (Baylor College of Medicine, Houston). rfx^{49} and rfx^{253} stocks were from B. Durand (Université Claude Bernard, Lyon, France). Other mutant and aberration stocks were obtained from the *Drosophila* stock center at Bloomington. Flies were raised on standard medium at 21°C–25°C. *nompB* was mapped relative to P element insertions in *l(2)02074* and *l(2)03832* by P-induced male recombination [32]. Male *Sp nompB cn bw/*Sp^{+} $nompB^{+}$ *P cn* bw^{+}*; Sb P{Δ2-3}99B/+* flies were crossed to *cn bw/Cy cn bw Roi* females. *Sp* bw^{+} *and* Sp^{+} *bw* recombinants were crossed to *nompB cn bw/CyO* and *Sp nompB cn bw/Cy cn bw Roi* flies, respectively. Multiple recombinant chromosomes were analyzed. Both P elements yielded *Sp nompB P cn* bw^{+}, and Sp^{+} $nompB^{+}$ *P cn bw* recombinants, therefore, lie centromere-proximal to the *nompB* mutation. The deficiency chromosome *Df(2L)03832MR1* also arose as a P-induced male recombinant derivative of *l(2)03832* [56].

Molecular Mapping and Sequencing

The genomic DNA flanking the distal breakpoint of *Df(2L)03832MR1* was isolated by single fly inverse polymerase chain reaction (PCR) [57] using the primer sets described by the *Drosophila* Genome Project (http://www.fruitfly.org/about/methods/inverse.pcr.html). The amplified fragments were sequenced by using the BigDye Terminator Cycle Sequencing Ready Reaction kit (PE Applied Biosystems).

The predicted transcript sequence was determined by amplifying and sequencing overlapping cDNA fragments. Polyadenylated RNA was isolated from adult *cn bw* flies by using Dynabeads (Dynal) and was reverse transcribed by Superscript II reverse transcriptase (GIBCO-BRL). Six overlapping cDNA fragments that include the entire coding sequence were amplified and sequenced. To sequence *nompB* mutant alleles, cDNA was made from flies heterozygous for each *nompB* allele and *Df(2L)03832MR1*. To determine the deletion in the $nompB^{1}$ chromosome, genomic DNA fragments from exon 1 to exon 5 were amplified from $nompB^{1}$*/Df(2L)03832MR1* flies with the Expand Long Template PCR System (Roche Applied Science) and were used for restriction enzyme digestion mapping.

DNA Constructs and Transformation

To make a genomic-cDNA fusion construct, a genomic DNA fragment extending 2.2 kb upstream from the translation start site was joined at an MluI site to cDNA including 127 base pairs of 5′-UTR, the entire coding sequence, and the polyadenylation signal. The genomic-cDNA fusion was cloned into the pPCaSpeR4 vector [58]. Both cDNA and genomic DNA were amplified from adult *cn bw* flies by using the Expand High Fidelity PCR System (Roche, Applied Science). To construct a GFP-*nompB* fusion gene, two fragments of the genomic-cDNA construct were amplified by PCR, to replace the translational start site with NheI and PvuII restriction enzyme sites, followed by sequence encoding the tripeptide spacer Ser-Gly-Gly. The NheI/ScaI-digested enhanced GFP (EGFP) (Clontech) cDNA was ligated to NheI/PvuII sites in the modified PCR products of the genomic-cDNA construct. The resulting genomic-cDNA fusion, encoding an EGFP-spacer-NOMPB fusion protein, was cloned into the P element transformation vector pPCaSpeR4. To make a Gal4-inducible *nompB* construct, the cDNA was inserted into the transformation vector pUAST. To remove the X box, a plasmid containing the cDNA was digested with EcoRV and MluI, treated with T4 DNA polymerase (GIBCO-BRL) to generate blunt ends, and self-ligated. The modified cDNA was then inserted into pUAST. Germline

transformation of a w^{1118} stock was carried out as described [59]; inserts were introduced into mutant backgrounds by genetic crosses.

Electrophysiological Recordings

Bristle mechanoreceptor currents were recorded with a saline-filled glass electrode placed over the cut end of thoracic macrochaetes as described previously [35]. Mechanical stimuli were given by moving the recording electrode and bristle 30 μm with a piezoelectric stage (Burleigh Instruments) at a transepithelial holding potential of 40 mV. Sound-evoked potentials were recorded from the antennal nerve with tungsten electrodes as described [30].

GFP Visualization and Antibody Staining

To examine the morphology of sensory neurons in campaniform sensilla, wings from *MJ94/+; nompB; UAS-GFP/+* or *MJ94/+; nompB/+; UAS-GFP/+* flies were dissected out, dry mounted, and observed under ultraviolet epifluorescence (Olympus BX60). To visualize adult chordotonal neurons, *elav-Gal4 CD8-GFP/+; nompB* or *elav-Gal4 CD8-GFP/+*; *nompB/+* flies were used. Pupal antennae and legs were dissected in PBS at 36–48 hr after puparium formation and were fixed in 4% formaldehyde for 1 hr at room temperature. After rinsing three times with PBS, tissues were mounted in 70% glycerol and observed under confocal microscopy (Zeiss LSM510).

To analyze GFP-NOMPB localization, tissues were dissected from GFP-NOMPB-expressing pupae, fixed as above, and washed with phosphate-buffered saline/0.2% Triton X-100 (PBT). After incubating with blocking solution (PBT with 5% normal goat serum and 5% bovine serum albumin) for 1 hr at room temperature, tissues were incubated with mAB 22C10 (1:20 dilution, Developmental Studies Hybridoma Bank, Iowa City, IA) in blocking solution overnight at 4°C. Tissues were then washed three times with PBT, incubated with Alexafluor 546-conjugated goat anti-mouse antibody (1:500 dilution, Molecular Probes) in blocking solution for 2 hr at room temperature, washed with PBT three times, rinsed in PBS, and mounted in 70% glycerol.

To analyze GFP-NOMPB localization in the embryo, embryos were fixed, manually devitellinized, and labeled with antibody as described above; however, 2% BSA and 2% NGS were used. Tissues labeled with antibody and GFP-NOMPB were examined by confocal microscopy (Leica DMIRE2). Scolopales were observed to emit autofluorescence under 492 nm, so a wavelength cutoff of 495 nm was used when imaging GFP fluorescence. Images were processed in Photoshop (Adobe, version 6.0).

Making Germline Clones

nompB alleles were recombined onto chromosomes bearing the *P{ry$^+$, neo^R, FRT40A}* insert by P element-induced recombination at the FRT insert site. Male *Sco$^+$ nompB cn bw/Sco P{ry$^+$, neo^R, FRT40A} cn$^+$ bw$^+$; Sb P{Δ2-3}99B/+* flies were crossed to *Sco cn bw/CyO* females. To select recombinants with intact FRT, progeny from crosses between *Sco$^+$ nompB P{?} cn$^+$ bw$^+$* recombinants and *Sp nompB cn bw/Cyo* flies were grown on media containing G418 [60]. Three *nompB^2 FRT* and two *nompB^3 FRT* chromosomes were recovered.

To make a *DMS* FRT chromosome, females with the genotype of *w; P{HDM} Sco$^+$/Sco P{ ry$^+$, neo^R, FRT40A}* were crossed to *w/Y; Gla Bc/Cy cn bw Roi* males. *w; P{HDM} Sco P{ ry$^+$, neo^R, FRT40A}* and *w; P{HDM} Sco$^+$ P{ ry$^+$, neo^R, FRT40A}* recombinants were selected by eye color (*P{HDM}*carries *w$^+$*) and resistance to G418. Six recombinants were isolated.

To induce germline clones, heat shock-inducible flipases (hsFLP) on the X and third chromosomes were used; *P{HDM} Sco FRT/Cy cn bw Roi* or *hsFLP/FM7; P{HDM} Sco FRT/CyO* females were mated with *nompB FRT/Cy cn bw Roi; MKRS hsFLP Sb/+* or *hsFLP/Y; nompB FRT/CyO* males, respectively. The progeny from those crosses were incubated for 2 hr at 37°C each day during larval and pupal development, and resulting *hsFLP*-bearing *nompB FRT/ P{HDM} Sco FRT* males were crossed to *Sp Df(2L)03832MR1/CyO* females to test the production of germline clones and the function of *nompB* in spermatogenesis.

Sperm Competition Assay

One- or two-day-old *w* virgin females were mated en masse with one- to three-day-old *w; Gla Bc/Cy cn bw Roi* males for 4 hr, then separated from the males and placed individually in separate vials. After 2 days, each female was mated overnight with two or three second males (Canton-S or *elav-Gal4/Y; nompB/Sp Df(2L)03832MR1; P{UAS-ΔX-nompB}/+*) and placed individually in separate vials. P_2 was calculated for each female as the ratio of progeny from the second male to total progeny.

Acknowledgments

We thank Hyangyee Oh and Dr. Mitzi Kuroda for providing stocks containing male sterile P{HDM} inserts and Drs. Bénédicte Durand and Anne Laurençon for *Rfx* mutant stocks and for valuable discussions. This work was funded by grants to M.J.K. from the National Institute for Deafness and Communicative Disorders and the Pew Scholars' Program in the Biomedical Sciences and by a Howard Hughes Undergraduate Research Fellowship to B.H.K.

Received: June 9, 2003
Revised: August 13, 2003
Accepted: August 13, 2003
Published: September 16, 2003

References

1. Kozminski, K.G., Johnson, K.A., Forscher, P., and Rosenbaum, J.L. (1993). A motility in the eukaryotic flagellum unrelated to flagellar beating. Proc. Natl. Acad. Sci. USA *90*, 5519–5523.
2. Kozminski, K.G., Beech, P.L., and Rosenbaum, J.L. (1995). The *Chlamydomonas* kinesin-like protein FLA10 is involved in motility associated with the flagellar membrane. J. Cell Biol. *131*, 1517–1527.
3. Piperno, G., and Mead, K. (1997). Transport of a novel complex in the cytoplasmic matrix of *Chlamydomonas* flagella. Proc. Natl. Acad. Sci. USA *94*, 4457–4462.
4. Huang, B., Rifkin, M.R., and Luck, D.J. (1977). Temperature-sensitive mutations affecting flagellar assembly and function in *Chlamydomonas reinhardtii*. J. Cell Biol. *72*, 67–85.
5. Marshall, W.F., and Rosenbaum, J.L. (2001). Intraflagellar transport balances continuous turnover of outer doublet microtubules: implications for flagellar length control. J. Cell Biol. *155*, 405–414.
6. Pazour, G.J., Wilkerson, C.G., and Witman, G.B. (1998). A dynein light chain is essential for the retrograde particle movement of intraflagellar transport (IFT). J. Cell Biol. *141*, 979–992.
7. Pazour, G.J., Dickert, B.L., and Witman, G.B. (1999). The DHC1b (DHC2) isoform of cytoplasmic dynein is required for flagellar assembly. J. Cell Biol. *144*, 473–481.
8. Deane, J.A., Cole, D.G., Seeley, E.S., Diener, D.R., and Rosenbaum, J.L. (2001). Localization of intraflagellar transport protein IFT52 identifies basal body transitional fibers as the docking site for IFT particles. Curr. Biol. *11*, 1586–1590.
9. Rosenbaum, J.L., and Witman, G.B. (2002). Intraflagellar transport. Nat. Rev. Mol. Cell Biol. *3*, 813–825.
10. Orozco, J.T., Wedaman, K.P., Signor, D., Brown, H., Rose, L., and Scholey, J.M. (1999). Movement of motor and cargo along cilia. Nature *398*, 674.
11. Culotti, J.G., and Russell, R.L. (1978). Osmotic avoidance defective mutants of the nematode *Caenorhabditis elegans*. Genetics *90*, 243–256.
12. Perkins, L.A., Hedgecock, E.M., Thomson, J.N., and Culotti, J.G. (1986). Mutant sensory cilia in the nematode *Caenorhabditis elegans*. Dev. Biol. *117*, 456–487.
13. Cole, D.G., Diener, D.R., Himelblau, A.L., Beech, P.L., Fuster, J.C., and Rosenbaum, J.L. (1998). *Chlamydomonas* kinesin-II-dependent intraflagellar transport (IFT): IFT particles contain proteins required for ciliary assembly in *Caenorhabditis elegans* sensory neurons. J. Cell Biol. *141*, 993–1008.
14. Collet, J., Spike, C.A., Lundquist, E.A., Shaw, J.E., and Herman, R.K. (1998). Analysis of osm-6, a gene that affects sensory cilium structure and sensory neuron function in *Caenorhabditis elegans*. Genetics *148*, 187–200.
15. Fujiwara, M., Ishihara, T., and Katsura, I. (1999). A novel WD40 protein, CHE-2, acts cell-autonomously in the formation of *C. elegans* sensory cilia. Development *126*, 4839–4848.
16. Signor, D., Wedaman, K.P., Orozco, J.T., Dwyer, N.D., Barg-

mann, C.I., Rose, L.S., and Scholey, J.M. (1999). Role of a class DHC1b dynein in retrograde transport of IFT motors and IFT raft particles along cilia, but not dendrites, in chemosensory neurons of living *Caenorhabditis elegans*. J. Cell Biol. *147*, 519–530.

17. Qin, H., Rosenbaum, J.L., and Barr, M.M. (2001). An autosomal recessive polycystic kidney disease gene homolog is involved in intraflagellar transport in *C. elegans* ciliated sensory neurons. Curr. Biol. *11*, 457–461.
18. Haycraft, C.J., Swoboda, P., Taulman, P.D., Thomas, J.H., and Yoder, B.K. (2001). The *C. elegans* homolog of the murine cystic kidney disease gene Tg737 functions in a ciliogenic pathway and is disrupted in osm-5 mutant worms. Development *128*, 1493–1505.
19. Swoboda, P., Adler, H.T., and Thomas, J.H. (2000). The RFX-type transcription factor DAF-19 regulates sensory neuron cilium formation in *C. elegans*. Mol. Cell *5*, 411–421.
20. Wheatley, D.N. (1995). Primary cilia in normal and pathological tissues. Pathobiology *63*, 222–238.
21. Pazour, G.J., and Rosenbaum, J.L. (2002). Intraflagellar transport and cilia-dependent diseases. Trends Cell Biol. *12*, 551–555.
22. Moyer, J.H., Lee-Tischler, M.J., Kwon, H.Y., Schrick, J.J., Avner, E.D., Sweeney, W.E., Godfrey, V.L., Cacheiro, N.L., Wilkinson, J.E., and Woychik, R.P. (1994). Candidate gene associated with a mutation causing recessive polycystic kidney disease in mice. Science *264*, 1329–1333.
23. Yoder, B.K., Richards, W.G., Sweeney, W.E., Wilkinson, J.E., Avener, E.D., and Woychik, R.P. (1995). Insertional mutagenesis and molecular analysis of a new gene associated with polycystic kidney disease. Proc. Assoc. Am. Physicians *107*, 314–323.
24. Taulman, P.D., Haycraft, C.J., Balkovetz, D.F., and Yoder, B.K. (2001). Polaris, a protein involved in left-right axis patterning, localizes to basal bodies and cilia. Mol. Biol. Cell *12*, 589–599.
25. Pazour, G.J., Baker, S.A., Deane, J.A., Cole, D.G., Dickert, B.L., Rosenbaum, J.L., Witman, G.B., and Besharse, J.C. (2002). The intraflagellar transport protein, IFT88, is essential for vertebrate photoreceptor assembly and maintenance. J. Cell Biol. *157*, 103–113.
26. Murcia, N.S., Richards, W.G., Yoder, B.K., Mucenski, M.L., Dunlap, J.R., and Woychik, R.P. (2000). The Oak Ridge Polycystic Kidney (orpk) disease gene is required for left-right axis determination. Development *127*, 2347–2355.
27. Pazour, G.J., Dickert, B.L., Vucica, Y., Seeley, E.S., Rosenbaum, J.L., Witman, G.B., and Cole, D.G. (2000). *Chlamydomonas* IFT88 and its mouse homologue, polycystic kidney disease gene tg737, are required for assembly of cilia and flagella. J. Cell Biol. *151*, 709–718.
28. Pazour, G.J., and Witman, G.B. (2003). The vertebrate primary cilium is a sensory organelle. Curr. Opin. Cell Biol. *15*, 105–110.
29. Kernan, M., Cowan, D., and Zuker, C. (1994). Genetic dissection of mechanosensory transduction: mechanoreception-defective mutations of *Drosophila*. Neuron *12*, 1195–1206.
30. Eberl, D., Hardy, R., and Kernan, M. (2000). Genetically similar transduction mechanisms for touch and hearing in *Drosophila*. J. Neurosci. *20*, 5981–5988.
31. Keil, T.A. (1997). Functional morphology of insect mechanoreceptors. Microsc. Res. Tech. *39*, 506–531.
32. Chen, B., Chu, T., Harms, E., Gergen, J.P., and Strickland, S. (1998). Mapping of *Drosophila* mutations using site-specific male recombination. Genetics *149*, 157–163.
33. Adams, M., Celniker, S.E., Holt, R.A., Evans, C.A., Gocayne, J.D., Amanatides, P.G., Scherer, S.E., Li, P.W., Hoskins, R.A., Galle, R.F., et al. (2000). The genome sequence of *Drosophila melanogaster*. Science *287*, 2185–2195.
34. Vandaele, C., Coulon-Bublex, M., Couble, P., and Durand, B. (2001). *Drosophila* regulatory factor X is an embryonic type I sensory neuron marker also expressed in spermatids and in the brain of *Drosophila*. Mech. Dev. *103*, 159–162.
35. Walker, R.G., Willingham, A.T., and Zuker, C.S. (2000). A *Drosophila* mechanosensory transduction channel. Science *287*, 2229–2234.
36. Chung, Y.D., Zhu, J., Han, Y., and Kernan, M.J. (2001). nompA encodes a PNS-specific, ZP domain protein required to connect mechanosensory dendrites to sensory structures. Neuron *29*, 415–428.
37. Das, A.K., Cohen, P.W., and Barford, D. (1998). The structure of the tetratricopeptide repeats of protein phosphatase 5: implications for TPR-mediated protein-protein interactions. EMBO J. *17*, 1192–1199.
38. Blatch, G.L., and Lassle, M. (1999). The tetratricopeptide repeat: a structural motif mediating protein-protein interactions. Bioessays *21*, 932–939.
39. Van Der Spuy, J., Kana, B.D., Dirr, H.W., and Blatch, G.L. (2000). Heat shock cognate protein 70 chaperone-binding site in the co-chaperone murine stress-inducible protein 1 maps to within three consecutive tetratricopeptide repeat motifs. Biochem. J. *345*, 645–651.
40. Cole, D.G. (2003). The intraflagellar transport machinery of *Chlamydomonas reinhardtii*. Traffic *4*, 435–442.
41. Ray, K., Perez, S.E., Yang, Z., Xu, J., Ritchings, B.W., Steller, H., and Goldstein, L.S. (1999). Kinesin-II is required for axonal transport of choline acetyltransferase in *Drosophila*. J. Cell Biol. *147*, 507–518.
42. Goldstein, L.S., and Gunawardena, S. (2000). Flying through the *Drosophila* cytoskeletal genome. J. Cell Biol. *150*, F63–F68.
43. Sarpal, R., and Ray, K. (2002). Dynamic expression pattern of kinesin accessory protein in *Drosophila*. J. Biosci. *27*, 479–487.
44. Hummel, T., Krukkert, K., Roos, J., Davis, G., and Klambt, C. (2000). *Drosophila* Futsch/22C10 is a MAP1B-like protein required for dendritic and axonal development. Neuron *26*, 357–370.
45. Durand, B., Vandaele, C., Spencer, D., Pantalacci, S., and Couble, P. (2000). Cloning and characterization of dRFX, the *Drosophila* member of the RFX family of transcription factors. Gene *246*, 285–293.
46. Dubruille, R., Laurencon, A., Vandaele, C., Shishido, E., Coulon-Bublex, M., Swoboda, P., Couble, P., Kernan, M., and Durand, B. (2002). *Drosophila* regulatory factor X is necessary for ciliated sensory neuron differentiation. Development *129*, 5487–5498.
47. Sarpal, R., Todi, S., Sivan-Loukianova, E., Shirolikar, S., Subramanyan, N., Raff, E.C., Erickson, J.W., Ray, K., and Eberl, D.F. (2003). *Drosophila* Kinesin Associated Protein (DmKap) interacts with the Kinesin II motor subunit Klp64D to assemble chordotonal sensory cilia but not sperm tails. Curr. Biol. *13*, 1687–1696.
48. Perotti, M.E., and Pasini, M.E. (1995). Glycoconjugates of the surface of the spermatozoa of *Drosophila melanogaster*: a qualitative and quantitative study. J. Exp. Zool. *272*, 311–318.
49. Phelps, C.B., and Brand, A.H. (1998). Ectopic gene expression in *Drosophila* using GAL4 system. Methods *14*, 367–379.
50. Price, C.S., Dyer, K.A., and Coyne, J.A. (1999). Sperm competition between *Drosophila* males involves both displacement and incapacitation. Nature *400*, 449–452.
51. Golic, K.G., and Lindquist, S. (1989). The FLP recombinase of yeast catalyzes site-specific recombination in the *Drosophila* genome. Cell *59*, 499–509.
52. Tates, A. (1971). Cytodifferentiation during Spermatogenesis in *Drosophila* (Leiden, The Netherlands: Rijksuniversiteit).
53. Fuller, M. (1993). Spermatogenesis. In The Development of *Drosophila melanogaster*, Volume 2, M. Bate and A. Martinez Arias, eds. (Cold Spring Harbor, NY: Cold Spring Harbor Laboratory Press), pp. 71–147.
54. Pitnick, S., Spicer, G.S., and Markow, T.A. (1995). How long is a giant sperm? Nature *375*, 109.
55. Miller, G.T., and Pitnick, S. (2002). Sperm-female coevolution in *Drosophila*. Science *298*, 1230–1233.
56. Preston, C., Sved, J., and Engels, W. (1996). Flanking duplications and deletions associated with P-induced male recombination in *Drosophila*. Genetics *144*, 1623–1638.
57. Gloor, G., and Engels, W. (1990). Single-fly preps for PCR. Drosoph. Inf. Serv. *71*, 148–149.
58. Thummel, C., and Pirrotta, V. (1992). Technical Notes: New pCasPeR P element vectors. *Drosophila* Information Service *71*, 150.
59. Rubin, G.M., and Spradling, A.C. (1982). Genetic transformation of *Drosophila* with transposable element vectors. Science *218*, 348–353.
60. Xu, T., and Rubin, G.M. (1993). Analysis of genetic mosaics in developing and adult *Drosophila* tissues. Development *117*, 1223–1237.